AJNR

Heterogeneity of Cerebral Blood Flow in Alzheimer Disease and Vascular Dementia

Takuya Yoshikawa, Kenya Murase, Naohiko Oku, Masao Imaizumi, Masashi Takasawa, Piao Rishu, Yasuyuki Kimura, Yoshitaka Ikejiri, Kazuo Kitagawa, Masatsugu Hori and Jun Hatazawa

AJNR Am J Neuroradiol 2003, 24 (7) 1341-1347
http://www.ajnr.org/content/24/7/1341

Heterogeneity of Cerebral Blood Flow in Alzheimer Disease and Vascular Dementia

Takuya Yoshikawa, Kenya Murase, Naohiko Oku, Masao Imaizumi, Masashi Takasawa, Piao Rishu, Yasuyuki Kimura, Yoshitaka Ikejiri, Kazuo Kitagawa, Masatsugu Hori, and Jun Hatazawa

BACKGROUND AND PURPOSE: **Alzheimer disease (AD) and vascular dementia (VaD) are the two major diseases that cause dementia, and early diagnosis is important. Single photon emission CT (SPECT) of cerebral blood flow (CBF) is used for the early detection of dementia and as an auxiliary method for follow-up. AD shows reduced posterior blood flow and VaD manifests reduced anterior blood flow on CBF SPECT images. We examined the usefulness of 3D fractal analysis of CBF SPECT images to objectively quantify the heterogeneity of CBF in patients with AD and VaD.**

METHODS: **Thirty-two patients with AD and 22 with VaD based on neuropsychologic tests and imaging findings, as well as 20 age-matched control subjects underwent technetium-99m hexamethyl propyleneamine oxime CBF SPECT. We then conducted statistical image processing by 3D fractal analysis on reconstructed data. Fractal dimension, an index of heterogeneity, was then calculated for the whole brain, as well as for the anterior and posterior regions of the brain. A higher fractal dimension indicates that the CBF SPECT image is uneven. The ratio of fractal dimension of the anterior region to fractal dimension of the posterior region (A/P ratio) was calculated. Heterogeneity of CBF was compared among the AD, VaD, and control groups.**

RESULTS: **Fractal dimensions of the AD, VaD, and control groups were 1.072 ± 0.179 (mean ± SD), 1.005 ± 0.156, and 0.806 ± 0.06, respectively. A significant difference of fractal dimension was noted between the control group and the two types of dementia ($P < .0001$); however, no significant difference was noted between the AD and VaD groups. The A/P ratios of the AD and VaD groups were significantly different (0.952 and 1.163, respectively; $P < .01$).**

CONCLUSION: **Analysis of CBF SPECT images quantitatively showed that the fractal dimension was significantly higher (indicating heterogeneity) in patients with AD and VaD when compared with age-matched control subjects. Comparison of the A/P ratio on CBF SPECT images between AD and VaD groups showed that the heterogeneity of CBF was posterior-dominant for AD and anterior-dominant for VaD. Thus, 3D fractal analysis enabled a simple and objective evaluation of the heterogeneity of CBF in patients with AD and VaD.**

Determination of the pathology of dementia and the guidelines for treatment is a very important issue because of the aging of our society. Alzheimer disease (AD) and vascular dementia (VaD) are the two major causes of dementia.

Positron emission tomography (PET) or single photon emission CT (SPECT) of cerebral blood flow (CBF) has been used by many authors to examine differences in the dynamics of cerebral circulation and metabolism between AD and VaD (1, 2). A study on the dynamics of cerebral circulation and metabolism in AD showed that reduced blood flow in the temporoparietal association area is common from the early stage before cerebral atrophy is noticeable (3–6). As dementia progresses, blood flow starts to decrease in the frontal lobe (7), while blood flow is relatively well preserved in the pons, primary motor cortex, primary visual cortex of the occipital lobe, basal ganglia, and thalamus. Studies on the relationship between reduced blood flow and pathologic changes of the posterior cortical association area (ranging from the temporal lobe to the parietal lobe) have also been reported (8). Measurement of glucose

Received January 3, 2003; accepted after revision March 14.

From the Departments of Internal Medicine and Therapeutics (T.Y., N.O., M.T., P.R., Y.K., K.K., M.H.), Allied Health Sciences (K.M.), Nuclear Medicine and Tracer Kinetics (M.I., J.H.), and Clinical Neuroscience (Y.I.), Osaka University Graduate School of Medicine, Suita City, Osaka, Japan.

Address reprint requests to Takuya Yoshikawa, MD, Department of Internal Medicine and Therapeutics, Osaka University Graduate School of Medicine (A8), 2–2, Yamadaoka, Suita City, Osaka, 565-0871, Japan; e-mail: yoshi@tracer.med.osaka-u.ac.jp

metabolism in the brain by means of PET has reportedly shown that glucose metabolism is decreased in the posterior cingulate gyrus before any other site in the very early stage of AD (9). There have also been many reports on the dynamics of the cerebral circulation and metabolism in VaD. According to one report on Binswanger disease, which is a clinical variant of VaD, PET has shown that CBF and the cerebral metabolic rate for oxygen are decreased in the white matter as well as in the cortex (10). In addition, a diffuse decrease of CBF was observed at SPECT (11), and reduced blood flow was also commonly seen in the frontal lobe (12, 13). In VaD, abnormalities tend to be detected with cognitive function tests that include parameters for evaluation of frontal lobe function (14). Namely, AD tends to present with posterior-predominant rather than anterior-predominant blood flow reduction, whereas VaD tends to conversely present with anterior-predominant rather than posterior-predominant blood flow reduction.

Although visual evaluation of normal tomograms is the primary method currently used for SPECT in the area of general clinical testing, this method lacks objectivity because it is heavily influenced by differences in image quality and the image display method, as well as by the judgment of the interpreter. It is difficult to establish a region of interest (ROI) in exactly the same location for all subjects in semiquantitative analysis methods that employ the ROI, which are frequently used for nuclear medicine as more objective indexes, because of differences in brain morphology. In addition, the territory of the ROI is limited, but evaluation of locations other than the ROI is impossible, and a subjective influence cannot be avoided during establishment of the ROI. Recent statistical methods for the analysis of functional images have allowed changes that were missed with conventional ROI analysis to be more easily detected. CBF can now be evaluated three-dimensionally by using 3D stereotactic surface projections (15) for the diagnosis of disease that involves dementia. One of the advantages of evaluation by statistical image analysis of 3D sterotactic surface projections is that sites of abnormal CBF and metabolism can be detected more objectively, since correction can be done for anatomic differences among patients, and patient data can be statistically compared with a normal data base on a voxel-by-voxel basis. In this study, we quantified the heterogeneity of CBF, separately from the blood flow distribution, by performing 3D fractal analysis of CBF SPECT images. The fractal dimension calculated by means of 3D fractal analysis was used as an objective index of the heterogeneity of CBF.

The heterogeneity of the distribution of a tracer can provide us with useful information on the functional status of organs and tissues. Fractal analysis is a mathematic tool for dealing with complex systems that have no characteristic length scale (scale invariant) (16). Scale-invariant systems are usually characterized by noninteger dimensions, which are termed fractal dimensions. Fractal geometry allows structures to be quantitatively characterized in geometric terms, even if their forms are irregular and fragmented, because it deals with the geometry of hierarchies and random processes. In this study, fractal analysis was used to assess the heterogeneity of SPECT images. This type of analysis is most useful for characterizing branching structures, such as the pulmonary airways and blood vessels (17, 18). Spatial changes of regional blood flow and metabolism in living organs are measurable by using fractal analysis with PET and SPECT (16, 19–20). The observed variance increases along with the number of subregions studied in an organ (16), and such resolution-dependent variance can be described with fractal analysis (16, 20–21). Biologic systems show considerable spatial and temporal heterogeneity, such as CBF, myocardial blood flow, and pulmonary blood flow (21–23). VaD due to small-vessel disease is fairly common and is hard to distinguish from AD (24, 25). In this study, we examined the use of 3D fractal analysis for objective evaluation of the heterogeneity of CBF in patients with AD or with VaD due to small-vessel disease.

Characteristics of the AD, VaD, and Control groups

Variable Characteristic	AD	VaD	Control
No. of patients	32	22	20
M/F	15/17	12/10	9/11
Age, y*	67.0 ± 10.3	71.2 ± 8.2	67.6 ± 11.3
MMSE score*	19.1 ± 5.8	23.6 ± 3.4	28.5 ± 1.2

* Data are the mean ± SD.

Methods

Subjects

The subjects consisted of 32 patients (15 men, 17 women) with AD (AD group), 22 patients (12 men, 10 women) with VaD (VaD group), and 20 age-matched controls (nine men, 11 women) (control group). The clinical characteristics of these three groups are shown in the Table . All of the subjects were right-handed. CBF SPECT was performed from June 2000 to June 2002. The National Institute of Neurologic and Communicative Disorders and Stroke–Alzheimer Disease and Related Disorders Association, or NINCDS-ADRDA, diagnostic criteria (26) were used to diagnose probable AD. A diagnosis of VaD was made in a comprehensive manner based on the diagnostic criteria proposed by the National Institute of Neurologic Disorders and Stroke–Association International pour la Recherse et l'Enseignement en Neuroscience (NINDS-AIREN) (27), and the criteria for subcortical VaD proposed by Erkinjuntti et al (28). The 22 patients with VaD were classified as having small-vessel disease based on head MR images that revealed small infarcts ranging from 3 to 15 mm in diameter (seen as low signal intensity on T1-weighted images and as high signal intensity on T2-weighted images) in the basal ganglia, thalamus, pons, and deep white matter. The control group consisted of 20 age-matched individuals who attended our outpatient clinic for investigation of headache or dizziness and underwent CBF SPECT, but who had no neuropsychiatric abnormalities and no abnormalities at CT or MR imaging. The Mini-Mental State Examination (MMSE) (29) was performed within 3 months of CBF SPECT for evaluation of cognitive function. Patients who could not undergo the intellectual function test because of conditions such as aphasia were excluded. Informed consent was obtained from all of the subjects and

from family members when a subject could not fully understand the details of the study.

Data Acquisition

Technetium-99m hexamethyl propyleneamine oxime (^{99m}Tc-HMPAO) was created by reconstituting HMPAO with 20 mCi (740 MBq) of fresh ^{99m}Tc pertechnetate. ^{99m}Tc-HMPAO was injected intravenously while the subject rested supine on the scanning bed with the eyes closed in a quiet examination room. SPECT scanning was performed with a four-headed gamma camera (Gamma View SPECT 2000H; Hitachi Medical Corp., Tokyo, Japan), by using a low-energy thin-section parallel-hole collimator (30). The in-plane and axial resolution after reconstruction was 10.0 mm in full-width at half-maximum. SPECT acquisition was performed at 8 seconds per step, with 128 collections over 360°, and data were recorded in a 64 × 64 matrix.

The raw SPECT data were transferred to a nuclear medicine computer (HARP 3; Hitachi Medical Corp.). The projection data were prefiltered with a Butterworth filter (cutoff frequency 0.20 cycles/pixel, order 10) and reconstructed into transaxial sections of 4.0-mm-thick images in planes parallel to the orbitomeatal line. Chang's attenuation correction was applied to the reconstructed data by using an attenuation coefficient of 0.08 cm^{-}.

Anatomic Standardization

Anatomic standardization involves fitting individual brains of different sizes and shapes into the configuration of a standard brain with a fixed coordinate system. We used Neurologic Statistical Image Analysis Software (NEUROSTAT) developed by Minoshima et al (15) at the University of Washington to perform anatomic standardization of our SPECT data. First, the midsagittal plane was determined, and the brain angle was corrected for x plane, y plane, and z plane, since the original images obtained with SPECT are angled depending on the position at the time of imaging. Next, the anterior commissure–posterior commissure line, which is the reference line, was fixed based on four reference points (the polus frontalis, the base of the anterior aspect of the corpus callosum, the base of the thalamus, and the polus occipitalis) within the dimension and was matched to the standard brain coordinate system of Talairach and Tournoux (31). Then, linear transformation and nonlinear transformation were performed, and the brain surface was fitted to the contours of the standard brain by deformation. Since NEUROSTAT performs conversion three-dimensionally along the nerve fibers, atrophic brains could also be appropriately converted to the standard brain (32).

Three-Dimensional Fractal Analysis

In fractal geometry, the relationship between a measure (M) and the scale (a) is expressed as follows:

$$M(a) = k \cdot a^{-D}, \quad (1)$$

where k is a scaling constant and D is called the fractal dimension (17). As Equation 1 implies, the quantity $M(a)$ to be measured is a function of the ruler scale and can be a nonconstant. D is one parameter that is useful for this purpose in characterizing organizationally complex structures (33).

CBF SPECT was performed by using ^{99m}Tc-HMPAO, and the cutoff value for the maximal voxel radioactivity on reconstructed images was established by dividing it from 35% to 50% at 11 equal intervals. The number of voxels with radioactivity equal to or above the established cutoff values was calculated. The cutoff value of the maximal radioactivity was defined as a and the total number of voxels measured was defined as $M(a)$, as shown in Equation 1. The cutoff values were changed in sequential order as this process was repeated, and the number of voxels with radioactivity equal to or above the established cutoff values was calculated. Then, the relationship between the number of voxels with a radioactivity equal to or greater than the established cutoff values and each cutoff value was determined. Finally, the relationship between the number of voxels and the cutoff values was converted into natural logarithms and plotted as a linear relationship. The logarithmic cutoff values were plotted on the horizontal axis of a graph, and the logarithmic value of the number of voxels was plotted on the vertical axis. The slope of this line corresponded to the fractal dimension (Fig 1). A higher fractal dimension indicates that the CBF SPECT image is uneven. As shown in Figure 1, one representative CBF SPECT image each was selected from the AD group, the VaD group, and the control group, after which 3D fractal analysis was performed and the fractal dimension was calculated. The fractal dimensions for the AD case, the VaD case, and the control case were 1.320, 1.112, and 0.767, respectively.

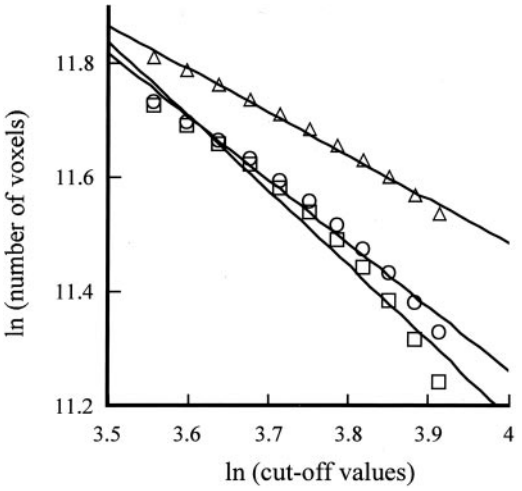

FIG 1. Method for calculating the fractal dimension in one representative case each from the AD group, the VaD group, and the control group. □ indicates AD patient ($y = -1.32x + 16.46$; $r = 0.994$); ○ indicates VaD patient ($y = -1.112x + 15.71$; $r = 0.992$); △ indicates age-matched control ($y = -0.767x + 14.55$; $r = 0.996$)

Items Examined

The fractal dimension of the whole brain was compared among the AD, VaD, and control groups. To examine the differences in CBF between the AD and VaD groups, the cerebrum was divided into anterior and posterior regions by a line connecting the central sulcus on the left and right sides, and the fractal dimension of each region was calculated. The borderline between the anterior region and the posterior region was determined by performing anatomic standardization so that the location did not vary from case to case. The ratio of fractal dimension of the anterior region to fractal dimension of the posterior region was calculated as an anterior-posterior ratio (A/P ratio) and was compared between the AD group and the VaD group.

Statistical Analysis

For comparison of the fractal dimension among the AD, VaD, and control groups, statistical analysis was performed by using the Mann-Whitney U test. The significance of differences in the clinical characteristics of these three groups was assessed with the Mann-Whitney U test. Statistical analysis was performed with the Wilcoxon signed rank test for comparison of the fractal dimension after the data for the AD group and the

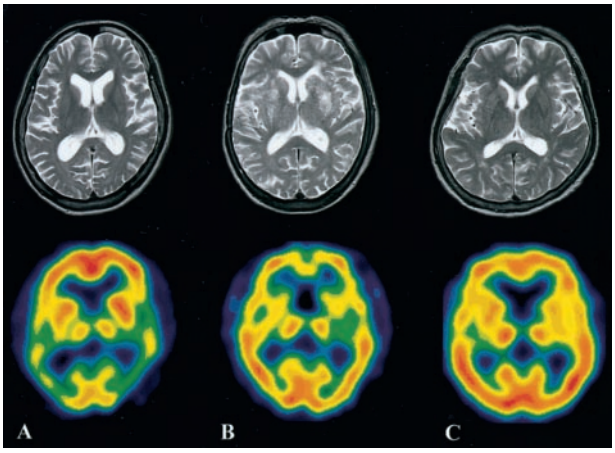

FIG 2. A representative case from each group (same cases as in Fig 1). Upper images are T2-weighted MR images; lower images are SPECT images.

A, A 69-year-old woman with AD. T2-weighted MR image does not show any clear abnormality. SPECT image shows blood flow reduction in the bilateral temporoparietal lobes.

B, A 67-year-old man with VaD. Multiple small infarcts are observed in the bilateral basal ganglia on the T2-weighted MR image. A frontal region decrease of CBF is noted on the SPECT image.

C, A 70-year-old female age-matched control subject.

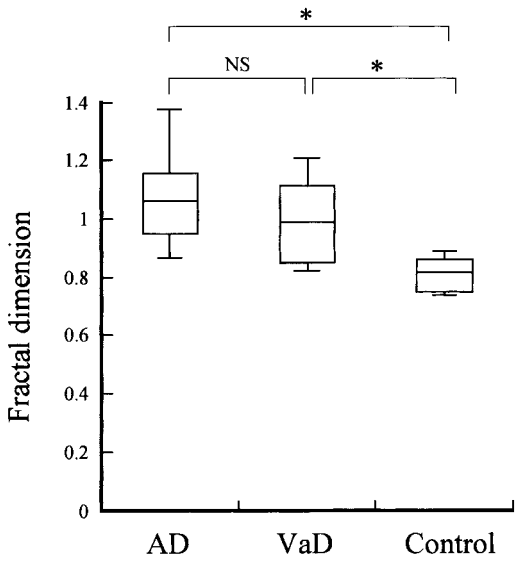

FIG 3. Comparison of fractal dimensions among the AD, VaD, and control groups. Statistical analysis by the Mann-Whitney *U* test showed significant differences (*$P < .0001$) between the control group and the AD group, as well as between the control group and the VaD group. However, no significant difference (*NS*) was noted between the AD group and the VaD group

VaD group were divided into anterior and posterior regions. Results are expressed as mean ± standard deviation (SD), and statistical significance was defined as a P value less than .01.

Results

There were no marked differences in age or sex among the three groups. The MMSE score of the AD group was 19.1 ± 5.8 (mean ± SD), which was lower compared with 23.6 ± 3.4 in the VaD group (Table). However, the result showed no significant difference.

T2-weighted MR images and SPECT images of a representative patient from each group are shown in Figure 2. Although the AD group did not show any clear abnormalities on the T2-weighted MR images, a decrease of CBF in the bilateral temporoparietal lobes was noted on SPECT images. In the VaD group, multiple small infarcts were observed in the bilateral basal ganglia on the T2-weighted MR images, and a frontal region decrease of CBF was noted on SPECT images. The representative cases in Figure 2 are the same as those displayed in Figure 1.

The fractal dimensions in the AD, VaD, and control groups were 1.072 ± 0.179 (mean ± SD), 1.005 ± 0.156, and 0.806 ± 0.06, respectively (Fig 3). The fractal dimension of the whole brain showed a statistically significant difference between the control group and the two groups with dementia ($P < .0001$). In contrast, no significant difference was noted between the AD and VaD groups. The whole brain was divided into anterior and posterior regions, and the fractal dimensions of each region were calculated for comparison between the AD group and the VaD group (Fig 4). In the AD group, the fractal dimension was significantly higher in the posterior region than in the anterior region ($P < .01$), which suggested the presence of posterior-predominant heterogeneity of CBF. In contrast, the VaD group showed a significantly higher fractal dimension in the anterior region than in the posterior region ($P < .01$), which suggested the presence of anterior-predominant heterogeneity of CBF. The A/P ratios of the AD group and the VaD group were 0.952 and 1.163, respectively.

Next, the A/P ratios and fractial dimension of the whole brain were plotted on the horizontal axis and vertical axis, respectively, and each patient in the AD group and the VaD group was examined (Fig 5). A horizontal line was drawn where the mean fractal dimension of the whole brain in the control group was 0.806, and a vertical line was drawn where the A/P ratio was 1 (ie, when the heterogeneity of the anterior region and the posterior region was comparable). Although there was some spread of the data, most points were above the above-mentioned horizontal line in both the AD group and the VaD group. In addition, the two diseases tended to be separated by the A/P ratio of 1, since the AD group tended to have a ratio of 1 or less, whereas the VaD group had a ratio of 1 or more.

Discussion

CBF SPECT may not have much diagnostic significance for VaD compared with degenerative dementia, since VaD is diagnosed with MR imaging in most cases. Although a decrease of CBF and metabolism is naturally observed at sites of infarcts and hemorrhage sites in VaD, a decrease of CBF and metabolism in the cortex that is not limited to such locations can also be seen in diaschisis, and this is why CBF SPECT might have some significance. In a CT study, Loeb et al (34) found no difference in the location or size of

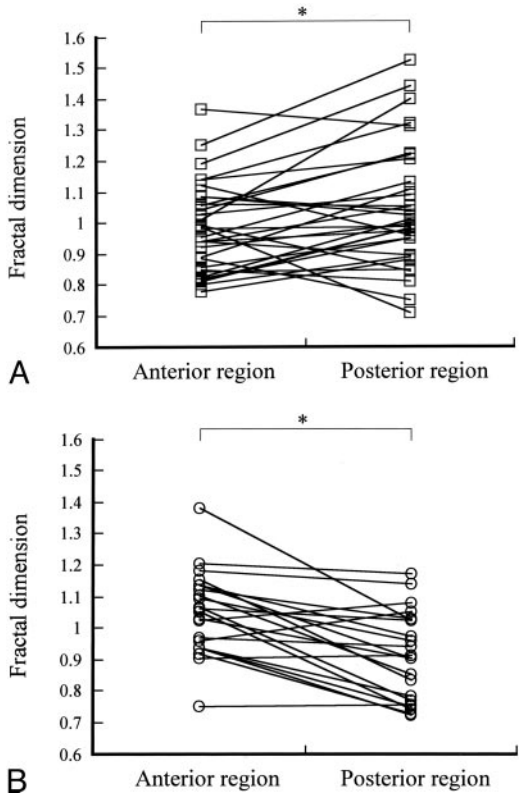

FIG 4. *A,* Fractal dimensions in the AD group plotted for the anterior region and the posterior region. Statistical analysis with the Wilcoxon signed rank test showed that the fractal dimension was significantly greater (*$P < .01$) in the posterior region than the anterior region in the AD group. A/P ratio = 0.952.

B, Fractal dimensions in the VaD group plotted for the anterior region and the posterior region. Statistical analysis with the Wilcoxon signed rank test showed that the fractal dimension was significantly greater (*$P < .01$) in the anterior region than the posterior region in the VaD group. A/P ratio = 1.163

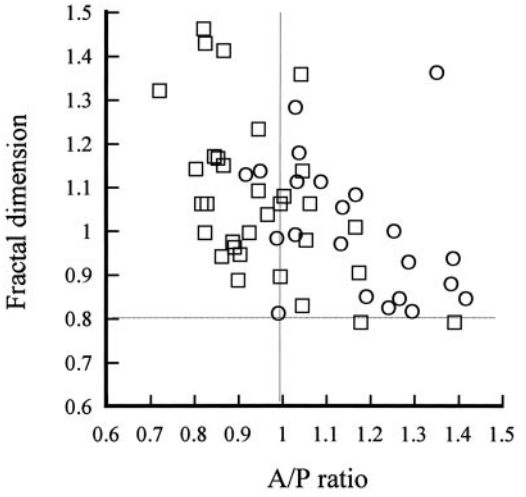

FIG 5. Relationship between the fractal dimension and the A/P ratio in the AD group and the VaD group. Horizontal line is mean fractal dimension of 0.806 for the control group; vertical line is A/P ratio of 1. Examination of individual cases of AD and VaD showed that these diseases tended to be separated by an A/P ratio of 1. □ indicates AD patients (n = 32); ○, VaD patients (n = 22)

infarcts between a group with dementia and a group without dementia, and they concluded that the morphologic findings on images should be evaluated cautiously. The properties, locations, and clinical features of brain lesions that cause VaD vary markedly from case to case. Therefore, when clinical studies are performed, results may not necessarily be uniform whatever diagnostic criteria are used. For the VaD group in this study, we selected patients with subcortical ischemia, which is relatively common and difficult to differentiate from AD by visual evaluation (24, 25). The primary brain lesions in this pathologic condition are lacunar infarcts due to the small-vessel disease and ischemic white matter lesions. The criteria for subcortical VaD proposed by Erkinjuntti et al (28) were used as the diagnostic criteria. These criteria were established by correcting the subcortical section of the NINDS-AIREN diagnostic criteria for VaD. The reason why blood flow reduction was observed in VaD due to small-vessel disease, even in the cortex where there were no morphologic abnormalities, seemed to be because cerebral circulation and metabolism were decreased as a secondary effect due to disconnection between the deep cerebrum and the cortex (35).

We performed 3D fractal analysius in the AD, VaD, and control groups and compared fractal dimensions for the whole brain. Our results quantitatively showed that there was heterogeneity of CBF in the AD group and the VaD group compared with the control group, whereas there was no quantitative difference in the heterogeneity of CBF between the AD group and the VaD group. When the whole brain was divided into an anterior region and a posterior region in these two groups and the fractal dimensions were calculated for each region, there was posterior-predominant heterogeneity of CBF in the AD group and there was anterior-predominant heterogeneity of CBF in the VaD group. This is a quantitative confirmation of previous reports suggesting that there is posterior-predominant blood flow reduction in AD versus anterior-predominant blood flow reduction in VaD (1, 2). However, we must be careful, as the fractal dimension is an index of the heterogeneity of CBF and not an index of the extent of blood flow reduction. For example, if blood flow and metabolism are maintained and the CBF distribution is uneven on normal visual evaluation, the fractal dimension will be high even if there is no reduction of blood flow.

In the AD group, some patients had higher fractal dimensions in the anterior region than in the posterior region when individual cases were examined. Since reduced anterior blood flow is also seen in frontotemporal dementia (36), care must be taken to differentiate between these diseases. Although the data are not presented here particularly, the A/P ratio for six cases of frontotemporal dementia was 1.482 ± 0.201(mean $\pm$ SD) and was much higher than the A/P ratio for VaD, suggesting the presence of anterior-predominant rather than posterior-predominant heterogeneity of CBF. Some patients with a frontal lobe–predominant reduction on PET scans and who receive a clinical diagnosis of AD may receive a di-

agnosis of frontotemporal dementia several years later. Blood flow reduction in the frontal lobe due to physiologic aging may also be a problem. The VaD group also had patients with a higher fractal dimension in the posterior region than in the anterior region. Since there are also mixed types of AD, it is not rare for AD to be associated with cerebrovascular disease. Examination of autopsy cases has shown that 35–39% of patients with AD also had brain infarction (37). Diagnosis of dementia at the level of MMSE score 20–25 is relatively difficult. The line separating deterioration of cognitive function due to so-called physiologic aging (age-related cognitive impairment) from mild cognitive impairment, which is thought to be a transitional stage toward early dementia, and the line separating mild cognitive impairment from dementia are still unclear (38, 39). Three-dimensional fractal analysis has limited the clinical application owing to the significant overlap in the fractal dimension and the A/P ratio by using fractal analysis in the AD group and the VaD group.

In this study, we performed 3D fractal analysis of CBF SPECT images to quantify the heterogeneity of CBF. Compared with SPECT, PET has superior sensitivity and resolution. Since images obtained by means of fluorine-18–2-fluoro-2-deoxy-D-glucose (^{18}F-FDG) have a better resolution than images obtained by using ^{15}O gas and $H_2{}^{15}O$, this method is widely used for investigation of AD. When correlation of the fractal dimension calculated from CBF SPECT images and ^{18}F-FDG PET images was examined before 3D fractal analysis was applied to CBF SPECT images, there was a significant correlation among the fractal dimensions obtained from each type of image, suggesting that heterogeneity of accumulation on CBF SPECT images was comparable to that on ^{18}F-FDG PET images (40, 41). On the basis of such findings, it seemed that the fractal dimension obtained with CBF SPECT might also reflect CBF and metabolism, and that SPECT can be used instead of PET at institutions that do not have a PET apparatus.

Kuikka et al (16, 42) calculated the fractal dimension as a measure of heterogeneity from the relationship between the relative dispersion (ie, the SD divided by the mean count) and the number of subregions. Although they determined the subregions semiautomatically, this does not appear to be a straightforward method, especially in 3D analysis. However, the 3D fractal analysis method is simple to perform in a 3D manner, does not need special software, and is objective. The most important factor in calculating the fractal dimension from SPECT images is the cutoff value. In this study, the cutoff value for the maximum radioactivity was set at 11 levels from 35% to 50% at equal intervals, and the number of voxels with radioactivity exceeding the cutoff value was calculated in each case. In all cases, the relationship between the cutoff value and the number of voxels (converted to a natural logarithm) was linear, and the correlation coefficient between them was 0.99, which suggested that the CBF SPECT image appeared to have a fractal form for this range of cutoff values and that the cutoff values used in this analysis were reasonable.

Since the shape of the brain varies from patient to patient, it is difficult to divide the brain into an anterior region and a posterior region at the same site in all cases. Also, there is a serious issue of how to divide the brain into an anterior region and a posterior region. Although the central sulcus might have been more accurately identified by placing a thin-section MR image with its extensive anatomic information over a CBF SPECT image, it has now become possible to solve this problem by standardizing the brain shape through conversion of a patient's SPECT images into the standard brain coordinate system of Talairach and Tournoux (31), after which the brain is divided into an anterior region and a posterior region at the line connecting the right and left central sulcus, which is easy to identify anatomically. Recently, statistical imaging has been used to assist in the diagnosis of dementia. Anatomic standardization is performed during this process. Since a common problem for statistical image analysis is the morphologic changes of a patient's brain, particularly the effects of cerebral atrophy, this must be taken into consideration. Because statistical methods can easily detect systemic differences of images, such as those due to imaging equipment and imaging conditions, unity of imaging methods is important.

Conclusion

The 3D fractal analysis method of statistical image analysis allows heterogeneity of CBF in AD and VaD to be quantified and may also allow a simpler and more objective evaluation.

Acknowledgments

We thank Messrs. Yukio Nakamura, Hiroaki Matsuzawa, Kouichi Fujino and Miss Tomoko Fukunaga for helping us to perform the nuclear medicine examinations and for evaluating cognitive function.

References

1. Frackowiak RS, Pozzilli C, Legg NJ, et al. **Regional cerebral oxygen supply and utilization in dementia: a clinical and physiological study with oxygen-15 and positron tomography.** *Brain* 1981;104: 753–778
2. Mielke R, Pietrzyk U, Jacobs A, et al. **HMPAO SPECT and FDG PET in Alzheimer disease and vascular dementia: comparison of perfusion and metabolic pattern.** *Eur J Nucl Med* 1994;21:1052–1060
3. Foster NL, Chase TN, Fedio P, et al. **Alzheimer disease: focal cortical changes shown by positron emission tomography.** *Neurology* 1983;33:961–965
4. Haxby JV, Gray CL, Koss E, et al. **Longitudinal study of cerebral metabolic asymmetries and associated neuropsychological patterns in early dementia of the Alzheimer type.** *Arch Neurol* 1990; 47:753–760
5. Jagust WJ, Friedland RP, Budinger TF, et al. **Longitudinal studies of regional cerebral metabolism in Alzheimer disease.** *Neurology* 1988;38:909–912
6. Holman BL, Johnson KA, Gerada B, et al. **The scintigraphic appearance of Alzheimer disease: a prospective study using technetium-99m-HMPAO SPECT.** *J Nucl Med* 1992;33:181–185

7. Ishii K, Sasaki M, Kitagaki H, et al. **Reduction of cerebellar glucose metabolism in advanced Alzheimer disease.** *J Nucl Med* 1997;38: 925–928
8. Bonte FJ, Weiner MF, Bigio EH, et al. **Brain blood flow in the dementias: SPECT with histopathologic correlation in 54 patients.** *Radiology* 1997;202:793–797
9. Minoshima S, Giordani B, Berent S, Frey KA, Foster NL, Kuhl DE. **Metabolic reduction in the posterior cingulate cortex in very early Alzheimer disease.** *Ann Neurol* 1997;42:85–94
10. Yao H, Sadoshima S, Kuwabara Y, Ichiya Y, Fujishima M. **Cerebral blood flow and oxygen metabolism in patients with vascular dementia of the Binswanger type.** *Stroke* 1990;21:1694–1699
11. Deutsch G, Tweedy JR. **Cerebral blood flow in severity-matched Alzheimer and multi-infarct patients.** *Neurology* 1987;37:431–438
12. Jagust WJ, Bundinger TF, Reed BR. **The diagnosis of dementia with single photon emission computed tomography.** *Arch Neurol* 1987;44:258–262
13. Starkstein SE, Sabe L, Vazquez S, et al. **Neuropsychological, psychiatric, and cerebral blood flow findings in vascular dementia and Alzheimer disease.** *Stroke* 1996;27:408–414
14. Wolfe N, Linn R, Babikian VL, Knoefel JE, Albert ML. **Frontal systems impairment following multiple lacunar infarcts.** *Arch Neurol* 1990;47:129–132
15. Minoshima S, Frey KA, Koeppe RA, Foster NL, Kuhl DE. **A diagnostic approach in Alzheimer disease using three-dimensional stereotactic surface projections of fluorine-18-FDG PET.** *J Nucl Med* 1995;36:1238–1248
16. Kuikka JT, Tiihonen J, Karhu J, et al. **Fractal analysis of striatal dopamine re-uptake sites.** *Eur J Nucl Med* 1997;24:1085–1090
17. Mandebrot BB. *Fractal geometry of nature.* San Francisco: W. H. Freeman and Company; 1982:131–137
18. Weibel ER. **Fractal geometry: a design principle for living organisms.** *Am J Physiol* 1991;261:361–369
19. Kuikka JT, Bassingthwaighte JB, Henrich MM, Feinendegen LE. **Mathematical modeling in nuclear medicine.** *Eur J Nucl Med* 1991; 18:351–362
20. Kuikka JT, Yang J, Karhu J, et al. **Imaging the structure of the striatum: a fractal approach to SPECT image interpretation.** *Physiol Meas* 1998;19:367–374
21. Bassingthwaighte JB, King RB, Roger SA. **Fractal nature of regional myocardial blood flow heterogeneity.** *Circ Res* 1989;65:578–590
22. Barman SA, McCloud LL, Catravas JD, Ehrhart IC. **Measurement of pulmonary blood flow by fractal analysis of flow heterogeneity in isolated canine lungs.** *J Appl Physiol* 1996;81:2039–2045
23. Nagao M, Murase K, Kikuchi T, et al. **Fractal analysis of cerebral blood flow distribution in Alzheimer disease.** *J Nucl Med* 2001;42: 1446–1450
24. Tatemichi TK, Desmond DW, Paik M, et al. **Clinical determinants of dementia related to stroke.** *Ann Neurol* 1993;33:568–575
25. Meyer JS, Xu G, Thornby J, Chowdhury MH, Quach M. **Is mild cognitive impairment prodromal for vascular dementia like Alzheimer disease?** *Stroke* 2002;33:1981–1985
26. McKhann G, Drachman D, Folstein M, et al. **Clinical diagnosis of Alzheimer disease: report of the NINCDS-ADRDA Work Group under the auspices of Department of Health and Human Services Task Force on Alzheimer disease.** *Neurology* 1984;34:939–944
27. Roman GC, Tatemichi TK, Erkinjuntti T, et al. **Vascular dementia: diagnostic criteria for research studies: report of the NINDS-AIREN International Workshop.** *Neurology* 1993;43:250–260
28. Erkinjuntti T, Inzitari D, Pantoni L, et al. **Research criteria for subcortical vascular dementia in clinical trials.** *J Neural Transm Suppl* 2000;59:23–30
29. Folstein MF, Folstein SE, McHugh PR. **"Mini-mental state": a practical method for grading the cognitive state of patients for the clinician.** *J Psychiatr Res* 1975;12:189–198
30. Kimura K, Hashikawa K, Etani H, et al. **A new apparatus for brain imaging: four-head rotating gamma camera single photon emission computed tomograph.** *J Nucl Med* 1990;31:603–609
31. Talairach J, Tournoux P: **Co-planar stereotaxic atlas of the human brain, three-dimensional proportional system: an approach to cerebral imaging.** New York: translated by Rayport M. Thieme Medical Publishers, Inc.; 1988
32. Minoshima S, Koeppe RA, Frey KA, et al. **Anatomic standardization: linear scaling and nonlinear warping of functional brain images.** *J Nucl Med* 1994;35:1528–1537
33. Nelson T. **Fractal physiologic complexity, scaling, and opportunities for imaging.** *Invest Radiol* 1990;25:1140–1148
34. Loeb C, Gandolfo C, Croce R, Conti M. **Dementia associated with lacunar infarction.** *Stroke* 1992;23:1225–1229
35. Hatazawa J, Shimosegawa E, Satoh T, Toyoshima H, Okudera T. **Subcortical hypoperfusion associated with asymptomatic white matter lesions on magnetic resonance imaging.** *Stroke* 1997;28: 1944–1947
36. The Lund and Manchester Groups. **Clinical and neuropathological criteria for frontotemporal dementia.** *J Neurol Neurosurg Psychiatry* 1994;57:416–418
37. Snowdon DA, Greiner LH, Mortimer JA, et al. **Brain infarction and the clinical expression of Alzheimer disease: the nun study.** *JAMA* 1997;277:813–817
38. Ritchie K, Touchon J. **Mild cognitive impairment:conceptual basis and current nosological status.** *Lancet* 2000;355:225–228
39. Kogure D, Matsuda H, Ohnishi T, et al. **Longitudinal evaluation of early Alzheimer disease using brain perfusion SPECT.** *J Nucl Med* 2000;41:1155–1162
40. Herhoz K, Schopphoff H, Schmidt M, et al. **Direct comparison of spatially normalized PET and SPECT scans in Alzheimer disease.** *J Nucl Med* 2002;43:21–26
41. Yoshikawa T, Murase K, Oku N, et al. **Statistical image analysis of cerebral blood flow in vascular dementia with small vessel disease.** *J Nucl Med* 2003;44:505–511
42. Kuikka JT, Hartikainen P. **Heterogeneity of cerebral blood flow: a fractal approach.** *Nuklearmedizin* 2000;39:37–42